Inorg. Chem. **1994,** *33,* 2857–2864

Models for the Molybdenum(VI/V) Centers of the Molybdenum Hydroxylases and Related Enzymes. Geometry, Electronic Structure, and EPR g-Tensor Predictions from *ab Initio* and Semiempirical Molecular Orbital Studies

Gang Peng,[1a,b] Jeff Nichols,[1c] Edward A. McCullough, Jr.,*,[1a] and Jack T. Spence[1a]

Department of Chemistry and Biochemistry, Utah State University, Logan, Utah 84322-0300, and
Utah Supercomputing Institute and Department of Chemistry, University of Utah,
Salt Lake City, Utah 84112

Received September 29, 1993[•]

The geometries and electronic structures of several molybdenum(V) and molybdenum(VI) complexes with tetradentate N_2S_2 and N_2O_2 ligands (LH_2 = *N,N'*-bis(2-mercaptophenyl)-*N,N'*-dimethyl-1,2-diaminoethane, *N,N'*-bis(2-hydroxyphenyl)-*N,N'*-dimethyl-1,2-diaminoethane) which have been proposed as models for the molybdenum(VI/V) centers of the molybdenum hydroxylases and related enzymes have been predicted using *ab initio* and INDO molecular orbital methods. *Ab initio* and INDO geometrical predictions have been compared with known X-ray crystal structures for three complexes and have been found to be in excellent agreement. In addition, the EPR **g** tensors of the molybdenum(V) complexes have been estimated using INDO methods. The results support previously proposed structures for both the model complexes and the enzyme molybdenum centers and are in good agreement with EPR and EXAFS experimental data for these systems. The results indicate the ligand has a profound effect on the geometry and electronic structures of the complexes. Insight into the electronic factors responsible for the EPR parameters of the complexes is presented, and application to the enzyme molybdenum centers is explored.

Introduction

Molybdenum hydroxylases[2] and related enzymes catalyze two-electron redox processes in which an oxygen atom or a hydroxyl group is formally added to or removed from the substrate. The best studied examples of these enzymes are xanthine oxidase (XO),[3a] xanthine dehydrogenase (XDH),[4a] sulfite oxidase (SO),[3a] and nitrate reductase (NR).[3b] Minimal structures of the oxidized molybdenum centers, as deduced by EXAFS and EPR, are $Mo^{VI}O(S)(SR)_2$ for XO[4] and XDH[4] and $Mo^{VI}O_2(SR)_{2-3}$ for SO[4a,f] and NR[4a] (*Chlorella vulgaris*). Additional oxygen or nitrogen ligands may be present,[4] while the thiolate ligands (SR) appear to be part of a cofactor (MoCo), common to all such enzymes.[5] The molybdenum centers cycle among the VI, V, and IV oxidation states, generating what are believed to be (omitting SR ligands) $Mo^{IV}O(SH)$ (XO, XDH) and $Mo^{IV}O(OH)$ (SO, NR) centers initially[4a–c,f] which, upon one-electron reoxidation, give EPR signals attributed to $[Mo^{V}OS]$,[4d] $[Mo^{V}O(SH)]$,[4a,b] and $[Mo^{V}O(OH)]$ centers,[3,4a,f,6] respectively. The inorganic biochemistry of these enzymes was recently reviewed.[7,8]

Considerable support for these structures was recently obtained from studies of analogue Mo^{VI}–dioxo complexes with tetradentate N_2S_2 and N_2O_2 ligands.[7–11] These complexes, for which several X-ray crystal structures are known,[9,12] undergo reversible one-electron reduction, generating $[Mo^{V}O_2L]^-$, $[Mo^{V}OSL]^-$, *cis*-$Mo^{V}O(OH)L$, and *cis*-$Mo^{V}O(SH)L$ species in solution.[9,13] In one case, solid complexes, formulated as $[Ph_4P][Mo^{V}OSL]$ and *trans*-$Mo^{V}O(SH)L$, have been isolated,[13] and the X-ray crystal structure of a closely related complex, *cis*-$Mo^{V}O(OSi(Me)_3)L$, has been obtained.[14] The EPR spectra of these complexes have been extensively investigated at multiple frequencies, and $^{95,97}Mo$,[9] ^{1}H,[9] ^{17}O,[14] and ^{33}S[11] coupling constants have been measured. In many cases, remarkable agreement with both g values and coupling constants for the enzymes has been observed.[9,11,14] These results provide compelling evidence, e.g., that $[Mo^{V}OS]$ and $[Mo^{V}O(SH)]$ are the sources of the very rapid and rapid EPR signals of XO.[7,8,11]

The $[Mo^{V}O_2L]^-$ species exhibit highly anisotropic frozen-solution EPR spectra, with extremely low $\langle g \rangle$ values.[9,10] At X-band, e.g., $\langle g \rangle \approx 1.90$, with anisotropy ($g_1 - g_3 > 300$ G). Replacement of an oxo ligand with a sulfido (thio) ligand reduces the anisotropy and raises the g values ($g_1 - g_3 \approx 200$ G, $\langle g \rangle \approx 1.96$).[9] Protonation to give *cis*-$Mo^{V}O(OH)L$ also reduces the anisotropy, while protonation of $[Mo^{V}OSL]^-$ to give *cis*-$Mo^{V}O(SH)L$ further reduces the anisotropy of this complex and raises $\langle g \rangle$ still higher (≈ 1.98).[9] Similar results are observed with XO

[•] Abstract published in *Advance ACS Abstracts,* May 15, 1994.

(1) (a) Utah State University. (b) Current address: Department of Applied Science, University of California, Davis, CA 95616. (c) University of Utah. Current address: Molecular Sciences Software Group, Pacific Northwest Laboratory, Richland, WA 99352.

(2) Also known as molybdenum oxotransferases or pterin-containing molybdenum enzymes.

(3) (a) Hille, R.; Massey, V. In *Molybdenum Enzymes*; Spiro, T. G.; Ed.; John Wiley: New York, 1985; p 443. (b) Adams, M. W. W.; Mortenson, L. E. *Ibid*, p 519.

(4) (a) Cramer, S. P. *Adv. Inorg. Bioinorg. Mech.* **1983,** *2,* 259. (b) Cramer, S. P.; Wahl, R. C.; Rajagopalan, K. V. *J. Am. Chem. Soc.* **1981,** *103,* 7721. (c) George, G. N.; Bray, R. C.; Cramer, S. P. *Biochem. Soc. Trans.* **1986,** *14,* 651. (d) Bray, R. C.; George, G. N. *Ibid.* **1985,** *13,* 560. (e) Bray, R. C.; Gutteridge, S.; Storter, D. A.; Tanner, S. J. *Biochem. J.* **1979,** *177,* 357. (f) Bray, R. C. *Polyhedron* **1986,** *5,* 591.

(5) Johnson, J. L.; Hainline, B. E.; Rajagopalan, K. V.; Anson, B. H. *J. Biol. Chem.* **1989,** *259,* 5414. Hawkes, T. R.; Bray, R. C. *Biochem. J.* **1984,** *219,* 481. Rajagopalan, K. V. *Adv. Enzymol. Relat. Areas Mol. Biol.* **1991,** *64,* 215.

(6) Bray, R. C. *Adv. Enzymol. Relat. Areas. Mol. Biol.* **1980,** *51,* 107.

(7) Bray, R. C. *Q. Rev. Biophys.* **1988,** *21,* 299.

(8) Enemark, J. H.; Young, C. G. *Adv. Inorg. Chem.*, submitted for publication. *Molybdenum enzymes, cofactors, and model systems*; Stiefel, E. I., Coucouvanis, D., Newton, W. E., Eds.; ACS Symposium Series 535; American Chemical Society: Washington, DC, 1993.

(9) Dowerah, D.; Spence, J. T.; Singh, R.; Wedd, A. G.; Wilson, G. L.; Farchione, F.; Enemark, J. H.; Kristofzski, J.; Bruck, M. *J. Am. Chem. Soc.* **1987,** *109,* 5655.

(10) Farchione, F.; Hanson, G. R.; Rodrigues, C. G.; Bailey, T. G.; Bagchi, R. N.; Bond, A. M.; Pilbrow, J. R.; Wedd, A. G. *J. Am. Chem. Soc.* **1986,** *108,* 831.

(11) Wilson, G. L.; Greenwood, R. J.; Pilbrow, J. R.; Spence, J. T.; Wedd, A. G. *J. Am. Chem. Soc.* **1991,** *113,* 6803.

(12) Hinshaw, C. J.; Peng, G.; Singh, R.; Spence, J. T.; Enemark, J. H.; Bruck, M.; Kristofzski, J.; Merbs, S. L.; Ortega, R. B.; Wexler, P. A. *Inorg. Chem.* **1989,** *28,* 4483.

(13) Singh, R.; Spence, J. T.; George, G. N.; Cramer, S. P. *Inorg. Chem.* **1989,** *28,* 8.

(14) Wilson, G. L.; Kony, M.; Tiekink, E. R. T.; Pilbrow, J. R.; Spence, J. T.; Wedd, A. G. *J. Am. Chem. Soc.* **1988,** *110,* 6923.

0020-1669/94/1333-2857$04.50/0

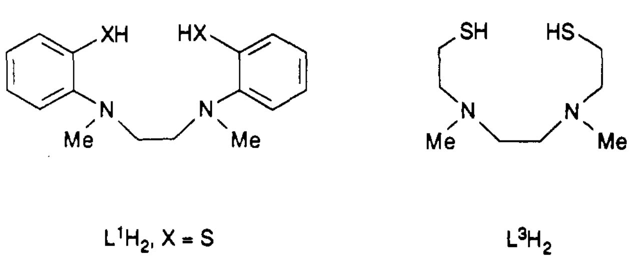

L^1H_2, X = S
L^2H_2, X = O

L^3H_2

Figure 1. Structures of ligands.

when the very rapid and rapid EPR signals are compared, although the absolute anisotropy is somewhat smaller.[7-11]

In order to obtain some insight into the electronic factors responsible for the remarkable EPR signals of the complexes, and to assist in the interpretation of the enzyme EPR signals, molecular orbital calculations have been performed on several of the complexes.

Molecular orbital calculations have been reported for a number of metal complexes, mainly those of first-row transition metals, and the results have been used to estimate EPR *g* values in several instances. The oxyhalides of Mo^V ($Mo^VOX_4^-$, e.g.), as well as a few dimeric and cluster compounds containing molybdenum, have been investigated by $X\alpha$–SW theory.[15-17] In the case of the oxyhalides, good agreement between experimental and calculated g tensors was found. Dithioline and dithiocarbamate complexes of molybdenum have been studied by extended Hückel theory,[18-21] while several clusters containing molybdenum have been investigated with Fenske–Hall theory.[22] Previous studies often have used known or assumed geometries, and we are unaware of any studies in which *ab initio* or semiempirical intermediate-neglect-of-differential overlap (INDO) calculations have been used to predict geometric structures of low-symmetry molybdenum complexes of the sizes reported here.

In this work, geometries, electronic energy levels, and, for Mo^V complexes, estimates of g tensors have been obtained using *ab initio* and INDO methods, for the complexes $Mo^{VI}O_2L^n$, $Mo^{VI}OSL^n$, $[Mo^VO_2L^n]^-$, $[Mo^VOSL^n]^-$, *cis*-$Mo^VO(OH)L^n$, *cis*-$Mo^VO(SH)L^n$, and *cis*-$Mo^VO(Otms)L^3$ (tms = trimethylsilyl). The analagous $Mo^VS(OH)L^n$ complexes were not investigated since this structure is not thought to be enzymatically relevant. Structures of the ligands are shown in Figure 1. The results have been used to interpret the EPR properties of the complexes. Applications to enzyme active site structures and EPR spectra have been explored.

Experimental Section

The synthesis and X-ray structures of $Mo^{VI}O_2L^n$ (n = 1, 2) and the EPR parameters of $[Mo^VO_2L^1]^-$, $[Mo^VOSL^1]^-$, *cis*-$Mo^VO(OH)L^1$, and *cis*-$Mo^VO(SH)L^1$ have been reported previously.[9] $[Mo^VO_2L^2]^-$, $[Mo^VOSL^2]^-$, *cis*-$Mo^VO(OH)L^2$, and *cis*-$Mo^VO(SH)L^2$ were generated in solution from $Mo^{VI}O_2L^2$ and their EPR spectra obtained by the same methods described for $Mo^{VI}O_2L^1$.[9,11,22] The synthesis, X-ray structure, and EPR spectra for $Mo^VO(Otms)L^3$ have been published.[14]

Single-configuration self-consistent-field (SCF) *ab initio* calculations were performed using a parallel version of the code DISCO.[23] For open-shell complexes a spin-restricted formalism was used. The code was modified slightly to eliminate convergence problems in these cases. The calculations were run on clusters of one to seven IBM RISC 6000 workstations in the Utah Supercomputing Institute and the Department of Chemistry at the University of Utah. For *ab initio* calculations on molecules of the sizes considered here, it is vitally important that the basis set be as small as possible. Two basis sets were employed in this work.

DISCO allows the use of generalized contractions,[24] so that in a minimum basis each atomic orbital may be represented by a single basis function, the SCF atomic orbital itself. Basis set A consists of this minimum set of SCF atomic orbitals on all ligand atoms; however, the 5s valence shell on Mo is split (5s, 5s′, 5p). Basis set B is derived from set A by further splitting the 4d shell on Mo and the valence s,p shells on ligand atoms. For the second-row atoms (S, Si) a set of 3d functions is added as well. Basis set details, including tables of the exponents and contraction coefficients, are given in the Appendix.

Other workers have shown that SCF-level calculations on $[MoS_nO_{4-n}]^{2-}$ anions with split valence basis sets comparable to our set B are quite successful in reproducing the experimental geometries of these complexes,[25] but these systems lack most of the peculiar features of our complexes: open shells, large size, low symmetry, unusually long Mo–N distances, and both singly and doubly bonded Mo–X (X = O, S). Accordingly, we believe the most convincing test of the adequacy of SCF-level calculations using our basis sets is the ability to reproduce known geometries of closely related complexes, especially open-shell complexes.

On a single workstation, *ab initio* calculations with the smallest basis required approximately 1 h per SCF iteration, with approximately 10–30 SCF iterations per geometry and 10–15 trial geometries per complex being required to converge bond lengths to 0.01 Å. In parallel, the code ran up to 5 times faster depending on the number of workstations and their percent utilization.

Semiempirical INDO calculations were performed with the code of Zerner and co-workers.[26] These also employed a spin-restricted formalism and are directly comparable to the corresponding *ab initio* calculations. We emphasize that we used the code as supplied and made no attempt to adjust any of the semiempirical parameters for our complexes. A complete INDO geometry optimization could be carried out in a few hours on a single workstation.

In the standard sum-over-states perturbation formulation, evaluation of the g tensor requires a knowledge of excited-state electronic energy levels and wave functions. Since the unoccupied orbitals in the open-shell SCF calculations do not correspond to true excited-state orbitals, or orbital energy differences to excitation energies, approximate excited states were calculated with INDO using single-excitation configuration-interaction (SCI) wave functions of the following form

$$\Psi = \sum_{f=1}^{p-1} c_f \Phi(f\rightarrow p) + \sum_{u=p+1} c_u \Phi(p\rightarrow u) \tag{1}$$

Here, $\Phi(f\rightarrow p)$ denotes a configuration in which a single electron has been excited from a doubly-occupied core (filled) orbital ϕ_f to the singly-occupied HOMO ϕ_p, doubly occupying the HOMO and leaving a hole in the core. Similarly, $\Phi(p\rightarrow u)$ denotes the excitation of an electron from the HOMO into a virtual (unoccupied) orbital. With a wave function of this form, for the computation of the g tensor it is possible to compress the entire expansion equation (1) into a single equivalent effective orbital ϕ' for each excited state:

$$\phi' = \sum_{u=p+1} c_u\phi_u - \sum_{f=1}^{p-1} c_f\phi_f \tag{2}$$

Test calculations which included the $f\rightarrow u$ excitations were performed on $[Mo^VO_2L^1]^-$ and $Mo^VO(OH)L^2$. Including these excitations greatly increased the number of configurations and complexity of the excited-state wave functions, but INDO excitation energies were changed by 10% or less. As there are already several approximations of comparable

---

(15) Thieren, M. J.; Trogler, W. C. *J. Am. Chem. Soc.* **1988**, *110*, 4942. Deeth, R. J. *J. Chem. Soc., Dalton Trans.* **1991**, 1895.

(16) Cook, M.; Karplus, M. *J. Chem. Phys.* **1985**, *83*, 6344.

(17) Cook, M.; Karplus, M. *J. Am. Chem. Soc.* **1985**, *107*, 257.

(18) Stiefel, E. I.; Eisenberg, R.; Rosenberg, R. C.; Gray, H. B. *J. Am. Chem. Soc.* **1966**, *88*, 2956.

(19) Stiefel, E. I.; Dori, Z.; Gray, H. B. *J. Am. Chem. Soc.* **1967**, *89*, 3353.

(20) Perkins, P. G.; Schultz, F. A. *Inorg. Chem.* **1982**, *21*, 3035.

(21) Perkins, P. G.; Schultz, F. A. *Inorg. Chem.* **1983**, *22*, 1133.

(22) Peng, G. Ph.D. Dissertation, Utah State University, 1989.

(23) Almlof, J.; Faegri, K.; Feyereisen, M.; Korsell, K. *DISCO, a direct ab initio code.* Private communication from M. Feyereisen. Almlof, J.; Faegri, K.; Korsell, K. *J. Comp. Chem.* **1982**, *3*, 385. Saebo, S.; Almlof, J. *Chem. Phys. Lett.* **1987**, *154*, 521.

(24) Dunning, T. H.; Hay, J. P. In *Methods of Electronic Structure Theory*; Schaefer, H. F., Ed.; Plenum: New York, 1977; p 1.

(25) Combariza, J. E.; Barfield, M.; Enemark, J. H. *J. Phys. Chem.* **1991**, *95*, 5463.

(26) Bacon, A. D.; Zerner, M. C. *Theor. Chim. Acta* **1979**, *53*, 21. Anderson, W. P.; Cundari, T. R.; Drago, R. S.; Zerner, M. C. *Inorg. Chem.* **1990**, *29*, 1.

Table 1. Selected Bond Lengths (Å)

	X-ray crystal structure	ab initio prediction (basis set)	INDO prediction
Mo^{VI}O$_2$L^1			
Mo–O$_{t1}$[a]	1.70	1.68 (B)	1.64
Mo–O$_{t2}$	1.70	1.68 (B)	1.64
Mo–S$_{\ell1}$[b]	2.41	2.49 (B)	2.42
Mo–S$_{\ell2}$	2.41	2.49 (B)	2.43
Mo–N$_1$	2.44	2.40 (B)	2.18
Mo–N$_2$	2.46	2.41 (B)	2.19
Mo^{VI}O$_2$L^2			
Mo–O$_{t1}$	1.70	1.69 (A)	1.64
Mo–O$_{t2}$	1.70	1.69 (A)	1.64
Mo–O$_{\ell1}$	1.96	1.98 (A)	1.97
Mo–O$_{\ell2}$	1.97	1.98 (A)	1.97
Mo–N$_1$	2.42	2.39 (A)	2.22
Mo–N$_2$	2.41	2.40 (A)	2.22
[Mo^{V}O$_2$L^1]$^-$			
Mo–O$_{t1}$		1.69 (B)	1.66
Mo–O$_{t2}$		1.69 (B)	1.66
Mo–S$_{\ell1}$		2.59 (B)	2.51
Mo–S$_{\ell1}$		2.61 (B)	2.53
Mo–N$_1$		2.46 (B)	2.21
Mo–N$_2$		2.48 (B)	2.22
[Mo^{V}O$_2$L^2]$^-$			
Mo–O$_{t1}$		1.87 (A) 1.89 (B)	1.88
Mo–O$_{t2}$		1.67 (A) 1.67 (B)	1.62
Mo–O$_{\ell1}$		2.09 (A) 2.10 (B)	2.06
Mo–O$_{\ell2}$		2.07 (A) 2.08 (B)	2.06
Mo–N$_1$[c]		2.51 (A) 2.51 (B)	2.25
Mo–N$_2$[d]		2.32 (A) 2.32 (B)	2.19
[Mo^{V}OSL^1]$^-$			
Mo–O$_t$			1.62
Mo–S$_t$			2.56
Mo–S$_{\ell1}$			2.47
Mo–S$_{\ell2}$			2.59
Mo–N$_1$			2.18
Mo–N$_1$			2.29
[Mo^{V}OSL^2]$^-$			
Mo–O$_t$			1.61
Mo–S$_t$			2.45
Mo–O$_{\ell1}$			2.04
Mo–O$_{\ell2}$			2.04
Mo–N$_1$			2.15
Mo–N$_2$			2.22
Mo^{V}O(OH)L^1			
Mo–O$_t$			1.63
Mo–OH			1.90
Mo–S$_{\ell1}$			2.43
Mo–S$_{\ell2}$			2.53
Mo–N$_1$			2.22
Mo–N$_1$			2.14
Mo^{V}O(OH)L^2			
Mo–O$_t$		1.67 (A)	1.62
Mo–OH		1.88 (A)	1.91
Mo–O$_{\ell1}$		1.99 (A)	1.95
Mo–O$_{\ell2}$		1.98 (A)	1.97
Mo–N$_1$[c]		2.40 (A)	2.24
Mo–N$_2$[e]		2.27 (A)	2.14
Mo^{V}O(SH)L^1			
Mo–O$_t$			1.63
Mo–SH			2.41
Mo–S$_{\ell1}$			2.42
Mo–S$_{\ell2}$			2.51
Mo–N$_1$			2.19
Mo–N$_2$			2.13
Mo^{V}O(SH)L^2			
Mo–O$_t$			1.63
Mo–SH			2.44
Mo–O$_{\ell1}$			1.93
Mo–O$_{\ell2}$			2.02
Mo–N$_1$			2.24
Mo–N$_2$			2.15
Mo^{V}O(Otms)L^3			
Mo–O$_t$	1.68	1.66 (B)	1.63
Mo–O$_{tms}$	1.91	1.88 (B)	1.81
Mo–S$_{\ell1}$	2.46	2.52 (B)	2.45
Mo–S$_{\ell2}$	2.41	2.52 (B)	2.46
Mo–N$_1$[c]	2.46	2.44 (B)	2.20
Mo–N$_2$[f]	2.29	2.26 (B)	2.17
Mo^{VI}OSL^1[g]			
Mo–O$_t$			1.61
Mo–S$_t$			2.15
Mo–S$_{\ell1}$			2.42
Mo–S$_{\ell2}$			2.41
Mo–N$_1$			2.19
Mo–N$_2$			2.13

[a] O$_t$, S$_t$ = terminal = O and S. [b] O$_\ell$, S$_\ell$ = ligand O and S. [c] Trans to short (oxo) Mo–O$_t$. [d] Trans to long Mo–O$_t$. [e] Trans to Mo–OH. [f] Trans to Otms (OSi(Me)$_3$). [g] Complex has not been synthesized or observed.

magnitude in our treatment of the g tensor, the computationally simpler equation (1) was used.

In all complexes except [Mo^{V}O$_2$L^2]$^-$, the unpaired electron is highly localized on just one atom k (Mo or S), so in calculating matrix elements of the spin–orbit operator, we make the further approximations of neglecting the atomic orbitals on all other atoms and replacing the operator with the atomic spin–orbit coupling constant times the orbital angular momentum operator. Then the EPR parameter g can be calculated using the equations

$$g^{\alpha,\beta} = g_e - 2\sum_n \frac{\langle\phi_p|l_k^\alpha|\phi_n'\rangle \zeta_k \langle\phi_n'|l_k^\beta|\phi_p\rangle}{\Delta E_n} \qquad (3)$$

where l_k is the orbital angular momentum operator centered on atom k, α and β are the x, y, and z orientations, p is the HOMO, ζ_k is the k atoms's spin–orbit coupling constant, g_e is the free-electron g value (2.0023), and ϕ_n' and ΔE_n are the effective orbital and excitation energy for excited state n. These equations are obtained from the standard second-order perturbation theory treatment of the g tensor.[27]

Although the formal oxidation state of Mo is V or VI, the theoretical calculations indicate that the actual charge on Mo in the complexes is approximately +2. For free Mo(II) Mabbs and Collison[28] suggest a spin–orbit coupling constant of 695 cm^{-1}. The multiplet average value derived from the gas-phase spectroscopy[29] of Mo^{2+} is 800 cm^{-1}. We used 746 cm^{-1}, the average of these. For S, we used 374 cm^{-1}, the value given by Mabbs and Collison and derived from gas-phase spectroscopy. These parameters were not adjusted to improve the agreement with experiment. A variation in ζ would lead to the same percentage variation in computed g-tensor anisotropy.

Results

Geometry of Complexes. Complete *ab initio* geometry optimizations were performed for six complexes: Mo^{V}O(Otms)L^3, Mo^{VI}O$_2$L^1, Mo^{VI}O$_2$L^2, [Mo^{V}O$_2$L^1]$^-$, [Mo^{V}O$_2$L^2]$^-$, and *cis*-Mo^{V}O(OH)L^2. The results are shown in Tables 1 and 2. Any error arising from the use of minimum basis sets for the ligand

---

(27) Stone, A. J. *Proc. R. Soc. London* **1963**, *A271*, 424. Beveridge, D. L. In *Semiempirical Methods of Electronic Structure Calculations*; Segal, G. A., Ed.; Plenum: New York, 1977; Part A.

(28) Mabbs, F. E.; Collison, D. *Electron Paramagnetic Resonance of d-Transition Metal Compounds*; Elsevier: Amsterdam, 1992.

(29) Sugar, J.; Musgrove, A. *J. Phys. Chem. Ref. Data* **1988**, *17*, 155.

Table 2. Selected Bond Angles (deg)

	X-ray crystal structure	*ab initio* prediction (basis set)	INDO prediction
$Mo^{VI}O_2L^1$			
$S_{\ell 1}$–Mo–$S_{\ell 2}$[a]	160	162 (B)	163
O_{t1}–Mo–N_2[b]	161	166 (B)	171
O_{t2}–Mo–N_1	158	164 (B)	166
O_{t1}–Mo–O_{t2}	107	101 (B)	100
N_1–Mo–N_2	75	76 (B)	77
$Mo^{VI}O_2L^2$			
$O_{\ell 1}$–Mo–$O_{\ell 2}$	151	154 (A)	151
O_{t1}–Mo–N_2	162	166 (A)	167
O_{t2}–Mo–N_1	161	165 (A)	166
O_{t1}–Mo–O_{t2}	108	102 (A)	102
N_1–Mo–N_2	74	73 (A)	76
$[Mo^VO_2L^1]^-$			
$S_{\ell 1}$–Mo–$S_{\ell 2}$		164 (B)	170
O_{t1}–Mo–N_2		162 (B)	165
O_{t2}–Mo–N_1		160 (B)	162
O_{t1}–Mo–O_{t2}		109 (B)	109
N_1–Mo–N_2		74 (B)	76
$[Mo^VO_2L^2]^-$			
$O_{\ell 1}$–Mo–$O_{\ell 2}$		157 (A) 156 (B)	154
O_{t1}–Mo–N_2		158 (A) 159 (B)	156
O_{t2}–Mo–N_1		173 (A) 173 (B)	176
O_{t1}–Mo–O_{t2}		102 (A) 101 (B)	101
N_1–Mo–N_2		73 (A) 74 (B)	76
$[Mo^VOSL^1]^-$			
$S_{\ell 1}$–Mo–$S_{\ell 2}$			158
S_t–Mo–N_2			136
O_t–Mo–N_1			147
S_t–Mo–O_t			79
N_1–Mo–N_2			72
$[Mo^VOSL^2]^-$			
$O_{\ell 1}$–Mo–$O_{\ell 2}$			155
O_t–Mo–N_2			174
S_1–Mo–N_1			158
O_1–Mo–S_t			96
N_1–Mo–N_2			79
$Mo^VO(OH)L^1$[c]			
$S_{\ell 1}$–Mo–$S_{\ell 2}$			161
O_{t1}–Mo–N_2			149
O_{t2}–Mo–N_1			165
O_{t1}–Mo–O_{t2}			93
N_1–Mo–N_2			75
$Mo^VO(OH)L^2$[c]			
$O_{\ell 1}$–Mo–$O_{\ell 2}$		161 (A)	155
O_{t1}–Mo–N_2		162 (A)	154
O_{t2}–Mo–N_1		169 (A)	178
O_{t1}–Mo–O_{t2}		104 (A)	104
N_1–Mo–N_2		76 (A)	77
$Mo^VO(SH)L^1$			
$S_{\ell 1}$–Mo–$S_{\ell 2}$			162
S_t–Mo–N_2			154
O_t–Mo–N_1			162
S_t–Mo–O_t			88
N_1–Mo–N_2			77
$Mo^VO(SH)L^2$			
$O_{\ell 1}$–Mo–$O_{\ell 2}$			153
S_t–Mo–N_2			154
O_t–Mo–N_1			167
S_t–Mo–O_t			91
N_1–Mo–N_2			76
$Mo^VO(Otms)L^3$[d]			
$S_{\ell 1}$–Mo–$S_{\ell 2}$	163	163 (B)	171
O_{t1}–Mo–N_1	162	168 (B)	161
O_{t2}–Mo–N_2	159	163 (B)	154
O_{t1}–Mo–O_{t2}	109	104 (B)	118
N_1–Mo–N_2	75	78 (B)	74
$Mo^{VI}OSL^1$[e]			
$S_{\ell 1}$–Mo–$S_{\ell 2}$			162
S_t–Mo–N_2			166
O_t–Mo–N_1			176
S_t–Mo–O_t			99
N_1–Mo–N_2			80

[a] O_ℓ, S_ℓ = ligand O and S. [b] O_t, S_t = terminal O and S. [c] O_{t1} = OH; O_{t2} = oxo. [d] Otms = OSi(Me)$_3$. [e] Complex has not been synthesized or observed.

atoms should be readily apparent in $[Mo^VO_2L^2]^-$, where the unpaired electron delocalizes to a significant extent onto one of the terminal O atoms. As can be seen, there is essentially no change in the predicted structure of this complex upon going from the minimum ligand basis A to the more flexible split valence set B. Consequently, only set A was used for the other two complexes containing the L^2 ligand. As explained in the Appendix, test calculations on small organosulfur molecules with basis sets of A quality gave poor results for distances to S, so only set B was used for sulfur-containing ligands.

Since the X-ray crystal structures of $Mo^VO(Otms)L^3$, $Mo^{VI}O_2L^1$, and $Mo^{VI}O_2L^2$ are known, a direct comparison with the predicted geometries is possible. To our knowledge, $Mo^VO(Otms)L^3$ is the only example of an open-shell Mo(V) complex with ligands closely related to L^1 and L^2 whose structure is known, so it provides an especially critical test of our approach. The *ab initio* results are in excellent agreement with the X-ray results for all three complexes. The small overestimation of bond distances to S seems to be typical of this level of theory; it was observed in the small-molecule test calculations with other basis sets as well.

The geometries of these six complexes also were predicted using INDO methods. As is seen in Tables 1 and 2, the INDO results, with the exception of the Mo–N(ligand) bond distances, are in excellent agreement with both the X-ray and *ab initio* results, and INDO is superior to *ab initio* for distances involving S. The geometry of $[Mo^VO_2L^1]^-$ is of particular interest because both INDO and *ab initio* methods predict that, in contrast to the cases of every other complex investigated one of the terminally-bonded atoms in the anion is not pushed out to a single-bond distance. The agreement between X-ray crystal structures and *ab initio* and INDO results indicates both *ab initio* and INDO methods may be used with some confidence to predict structures in these systems. Because of the great complexity of the calculations and the large amount of computer time required for the *ab initio* methods, INDO was used to predict structures for the remaining complexes (Tables 1 and 2).

The predicted structure for $Mo^{VI}OSL^1$ also is of considerable interest. While this species has neither been synthesized, nor observed *in situ*,[13] the $Mo^{VI}OS$ center appears to be present in oxidized xanthine oxidase.[7] The predicted structure has Mo–O and Mo–S bond lengths as anticipated for multiple oxo[12] and sulfido bonds;[30] they are also in excellent agreement with the bond lengths obtained from EXAFS data for the enzyme. It is important to note that the predicted Mo–S bond length (2.15 Å) is characteristic of a Mo–S bond order of 2,[30,31] while the corresponding Mo^V complex ($[Mo^VOSL^1]^-$) has a predicted bond length (2.56 Å) corresponding to a long Mo–S single bond.[9,12]

Electronic Structures (Energy Levels and Orbital Composition). In the calculation of the **g** tensor, the major contribution comes

---

(30) Young, C. G.; Enemark, J. H.; Collison, D.; Mabbs, F. E. *Inorg. Chem.* **1987**, *26*, 2925.

(31) Hofer, E.; Holzbach, W.; Wieghardt, K. *Angew. Chem., Int. Ed. Engl.* **1981**, *20*, 282.

Table 3. SCI Energy Levels[a,b] (cm^{-1})

	1st excited state	2nd excited state	3rd excited state
$[Mo^VO_2L^1]^-$	9 177	13 260	14 893
$[Mo^VO_2L^2]^-$	11 593, 10 853[c]	22 208, 21 110	54 609, 53 976
$[Mo^VOSL^1]^-$	7 896	18 061	35 188
$[Mo^VOSL^2]^-$	18 929	23 149	23 465
$Mo^VO(OH)L^1$	14 849	16 906	22 704
$Mo^VO(OHL^2$	19 247	20 462	31 237
$Mo^VO(SH)L_1$	15 415	16 892	23 730
$Mo^VO(SH)L^2$	16 575	17 858	25 157
$Mo^VO(Otms)L^3$	19 577	21 428	26 800

[a] All energies are with respect to the ground state. [b] Only the first three excited states contribute significantly to the g tensor. [c] Two values are for the two possible isomers (Mo–O_{t2} short, Mo–O_{t1} long; Mo–O_{t2} long, Mo–O_{t1} short).

Table 4. HOMO Atomic Orbital Coefficients[a]

$[Mo^VO_2L^1]^-$		$Mo^VO(OH)L^2$	
Mo p_x	0.23	Mo d_{z^2}	−0.08
Mo p_z	0.22	Mo $d_{x^2-y^2}$	0.16
Mo d_{z^2}	0.06	Mo d_{xy}	0.82
Mo d_{xy}	−0.56	Mo d_{xz}	0.20
Mo d_{yz}	−0.54	Mo d_{yz}	−0.18
$[Mo^VO_2L^2]^-$		$Mo^VO(SH)L^1$	
Mo d_{z^2}	0.17, 0.20[b]	Mo d_{z^2}	−0.20
Mo d_{xy}	0.14, 0.13	Mo $d_{x^2-y^2}$	−0.09
Mo d_{yz}	0.14, 0.09	Mo d_{xy}	0.70
O_{t1} p_x	0.65, 0.70	Mo d_{xz}	0.21
O_{t1} p_y	0.70, 0.65	Mo d_{yz}	−0.43
$[Mo^VOSL^1]^-$		$Mo^VO(SH)L^2$	
S_t p_x	−0.11	Mo d_{z^2}	−0.11
S_t p_y	0.44	Mo $d_{x^2-y^2}$	−0.10
S_t p_z	−0.85	Mo d_{xy}	0.76
$[Mo^VOSL^2]^-$		Mo d_{xz}	0.18
Mo d_{z^2}	0.71	Mo d_{yz}	−0.33
Mo $d_{x^2-y^2}$	−0.31	$Mo^VO(Otms)L^3$	
Mo d_{xy}	−0.37	Mo $d_{x^2-y^2}$	−0.32
Mo d_{xz}	0.12	Mo d_{xy}	−0.54
Mo d_{yz}	0.24	Mo d_{xz}	0.11
$Mo^VO(OH)L^1$		Mo d_{yz}	0.55
Mo s	0.10		
Mo p_z	0.07		
Mo d_{z^2}	0.21		
Mo d_{xy}	−0.65		
Mo d_{xz}	0.17		
Mo d_{yz}	0.51		

[a] For each complex, only those atomic orbitals are included which have a rounded coefficient of 0.1 or greater. [b] Values for the two isomers (see Table 3).

from the lowest two or three excited states. INDO excitation energies for these states are shown in Table 3. Given the many approximations, the precise values should not be taken too seriously; however, the trends probably are meaningful. Of particular interest are the very low-lying excited states predicted for $[Mo^VO_2L^2]^-$, $[Mo^VO_2L^1]^-$, and $[Mo^VOSL^1]^-$.

The INDO atomic orbital composition of the HOMO is given in Table 4. In all cases, the Mo 5p and 4d orbitals and the oxo 2p and sulfido 3p orbitals dominate the electronic structure. In other words, contributions from the ligand oxygen, sulfur, and nitrogen atoms are negligible. In the case of the ligand N atoms, the X-ray bond lengths (where known) are long,[9,12] indicating only weak Mo–N bonding exists, a manifestation of the well-known trans effect of an oxo ligand. In all Mo^V cases but two ($[Mo^VO_2L^2]^-$ and $[Mo^VOSL^1]^-$), the HOMO is composed predominantly of Mo 5p and 4d orbitals and the unpaired electron resides essentially on Mo. With $[Mo^VO_2L^2]^-$ the oxo O (long Mo–O_t bond) contributes significantly to the HOMO. With $[Mo^VOSL^1]^-$, the HOMO is composed almost entirely of sulfido S 3p orbitals, with the unpaired electron confined essentially to this S atom.

A precise interpretation of the individual atomic orbital coefficients is complicated by the fact that none of the complexes have any element of symmetry, so it is not possible to define Cartesian directions by reference to symmetry operations. Furthermore, the orientation of each complex is not preserved during the geometry optimization but changes in an essentially uncontrollable way. Taking the Mo as origin, in the protonated complexes the protonated O or S lies roughly on the *y* axis and the doubly-bonded O or S roughly on the *z* axis. Thus, the coefficients for these complexes are more or less directly comparable, and one sees that in terms of the atomic orbital character, the HOMOs are essentially identical. The orientation of $MoO(Otms)L^3$ differs primarily in that the O bonded to tms lies on the *x* and not the *y* axis. A 90° rotation about the *z* axis would interconvert these, which would interchange d_{xz} and d_{yz}, while the d_{xy} orbital, a dominant component of the HOMO in each of these complexes, would undergo at most a phase change.

Table 5. g Tensors

	g_{max}	g_{mid}	g_{min}	$\langle g\rangle$[a]
$[Mo^VO_2L^1]^-$				
calc	1.983	1.968	1.763	1.905
exp	1.986	1.912	1.811	1.901
$[Mo^VO_2L^2]^-$				
calc[b]				
exp	1.979	1.897	1.754	1.874
$Mo^VO(OH)L^1$				
calc	1.972	1.958	1.895	1.942
exp	1.981	1.944	1.944	1.957
$Mo^VO(OH)L^2$				
calc	1.968	1.966	1.921	1.952
exp	1.952	1.937	1.919	1.935
$[Mo^VOSL^1]^-$				
calc	2.002	1.971	1.919	1.964
exp	2.017	1.933	1.889	1.944
$[Mo^VOSL^2]^-$				
calc	1.972	1.968	1.887	1.942
exp	1.979	1.919	1.864	1.918
$Mo^VO(SH)L^1$				
calc	1.969	1.961	1.864	1.931
exp	2.016	1.961	1.954	1.979
$Mo^VO(SH)L^2$				
calc	1.968	1.963	1.899	1.943
exp	1.965	1.950	1.950	1.950
$Mo^VO(Otms)L^3$				
calc	1.979	1.971	1.898	1.949
exp[c]	(1.981)	(1.944)	(1.944)	1.947

[a] $\langle g\rangle$ exp obtained from room-temperature spectra; $\langle g\rangle$ calc is the average for *g* calc. [b] Not calculated because of extensive delocalization of the unpaired electron on both Mo and O_t. [c] $\langle g\rangle$ exp only reported. Anisotropic spectrum is reported to be superimposable on the anisotropic spectrum of *cis*-$Mo^VO(OH)L^1$. Values of g tensors for *cis*-$Mo^VO(OH)L^1$ in parentheses.

The final orientations of the anions are all similar, so the coefficients of these may also be compared; however, the orientations differ sufficiently from those of the protonated species to prohibit a direct comparison between the two groups. There is clearly much more variation in the HOMO in the anions.

g Tensors. Estimates of the g tensors have been made for all Mo^V complexes except $[Mo^VO_2L^2]^-$; results as well as experimental g tensors are found in Table 5. In our highly approximate treatment of the g tensor, the unpaired electron must primarily reside on a single atom with a large ζ. In the case of $[Mo^VO_2L^2]^-$, the *ab initio* and INDO calculations agree that the electron is delocalized to a significant degree on both the Mo and oxo O atoms. Attempts to force INDO to converge to a state with a localized electron were unsuccessful, and it seems clear that, at the INDO level of theory, no such localized state exists. While it is possible to take this delocalization into account, with molecules of low symmetry the calculation of the g tensor becomes extremely complicated and we have no computer code available to handle it. Unfortunately, this complex is in some ways the most interesting since it has the most anisotropic spectrum. It is significant that INDO calculations do predict a low-lying excited state for this complex, which is a necessary , but not a sufficient, condition for an anisotropic spectrum.

As discussed in the Introduction, the experimental **g** tensors for $[Mo^VO_2L^n]^-$ exhibit extremely large anisotropy.[9,22] The anisotropy of the $[Mo^VOSL^n]^-$ complexes is smaller, but still large.[9,22] Upon protonation of either species, the anisotroy is greatly reduced to that found for the vast majority of Mo^V oxo complexes reported in the literature. In general, this same pattern is found in the estimated values. In addition, the magnitudes of the calculated anisotropies ($g_{max} - g_{min}$) agree reasonably well with the magnitudes of the experimental anisotropies.

The calculated absolute values of the **g** tensors for the complexes with large anisotropy (the anions) agree remarkably well with the experimental values for the $\mathbf{g}_{max}$ and $\mathbf{g}_{min}$ tensors; in all cases, however, $\mathbf{g}_{mid}$ is significantly larger for the estimated values, with the **g** tensor pattern approaching that of an axial spectrum, rather than the highly rhombic experimental spectrum.[9,11,22] For the protonated species, considering the precision of the estimated **g**-tensor values, the agreement is remarkably good, except for *cis*-$Mo^VO(SH)L^1$ ($\mathbf{g}_{max}$ and $\mathbf{g}_{min}$ significantly lower for the estimated values). Unfortunately, only $\langle \mathbf{g} \rangle$ has been reported for $Mo^VO(Otms)L^3$, but this agrees very well with the estimated $\langle \mathbf{g} \rangle$ for this complex.[14] Also, the calculated **g** tensors are in good agreement with the experimental values for *cis*-$Mo^VO(OH)L^1$; the anisotropic EPR spectra for these two complexes are reported to be superimposable.[14]

Discussion

The ligand has a profound effect on the predicted structures of the Mo^V anion complexes. The X-ray crystal structures for both Mo^{VI} complexes indicate the Mo–O_t (O_t = terminal O) bonds have the normal bond length (~1.70 Å) expected for a multiple Mo–O_t bond. Addition of an electron to $Mo^{VI}O_2L^2$ to give $[Mo^VO_2L^2]^-$ results in a considerable lengthening of one Mo–O_t bond to a distance (1.87 Å) close to that for a Mo–O single bond (~1.90 Å). Addition of an electron to $Mo^{VI}O_2L^1$, however, gives $[Mo^VO_2L^1]^-$ with both Mo–O_t bonds having the normal Mo–O_t bond length (1.66 Å). Replacement of an oxo (O_t) with a sulfido (S_t) (S_t = terminal S) results in complexes with a slightly shorter Mo–O_t bond (1.61, 1.62 Å) and a greatly lengthened Mo–S_t bond (2.45, 2.56 Å; normal Mo–S single-bond length is 2.40–2.50 Å).[9,12]

The neutral (protonated) MO^V complexes and *cis*-$Mo^VO(Otms)L^3$ all have a Mo–O_t bond of normal length (1.62–1.63 Å) and a Mo–OH, Mo–SH, or Mo–Otms bond with a length expected for a single Mo–O or Mo–S bond (1.81–1.91 Å; 2.41–2.44 Å).[9,11,12]

The predicted structure for $Mo^{VI}OSL^1$ indicates the Mo–O_t and Mo–S_t bonds are both multiple (Mo=O_t and Mo=S_t), as expected for the oxidized complex and in agreement with bond lengths observed by EXAFS for the oxidized $Mo^{VI}OS$ center of xanthine oxidase.[3,4,7,8]

The electronic structures of the Mo^V anions are also affected by the ligand. While three of the anions have a small first excitation energy (compared to the neutral complexes), the unpaired electron is found in different molecular orbitals (HOMO), depending on the ligands. With $[Mo^VO_2L^2]^-$, the unpaired electron is delocalized extensively on Mo and one O_t (long Mo–O_t bond). The HOMO is composed of Mo 5p and 4d and O 2p orbitals with negligible contributions from the ligand orbitals. The HOMO for $[Mo^VO_2L^1]^-$ is composed primarily of Mo 4d and 5p orbitals, with a negligible contribution from any other atomic orbital (the HOMO is composed of ~71% Mo orbitals, with a total contribution of all other atomic orbitals of ~28%; in no case, however, does any single orbital contribute more than 1% to the 28%). Replacement of O_t with S_t gives $[Mo^VOSL^2]^-$ with a HOMO localized primarily on Mo (70% Mo 4d and 5p orbitals) with no significant contribution from any other single atomic orbital. For $[Mo^VOSL^1]^-$, the electron is localized almost entirely on S_t (92% S 3p orbitals). These results for the anions may be represented approximately as shown in Figure 2. For $[Mo^VO_2L^2]^-$, the HOMO appears to be a Mo–O_t π antibonding orbital centered mainly on O (the long Mo–O_t bond indicates a Mo–O_t bond order near 1). The HOMO for $[Mo^VO_2L^1]^-$, on the other hand, is probably a Mo d nonbonding atomic orbital, since both Mo–O_t bonds are multiple. With $[Mo^VOSL^2]^-$, the HOMO appears to be a Mo–S_t π antibonding orbital (the Mo–S_t bond order is ~1), centered mainly on Mo, while the HOMO for $[Mo^VOSL^1]^-$ is likely a Mo–S_t π antibonding orbital (the Mo–S_t bond length is that of a very long Mo–S single bond), which is almost entirely centered on S. The exceptionally long Mo–S_t bond length in this case may be a result of the effective localization of the electron on S.

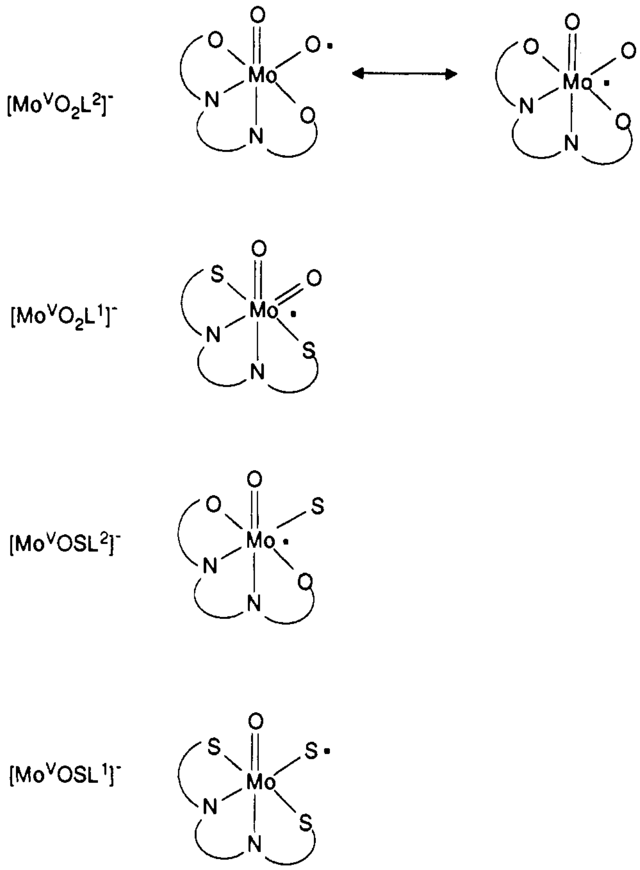

Figure 2. Approximate electronic structures of anions. A dot represents an unpaired electron.

For the protonated Mo^V complexes and $Mo^VO(Otms)L^3$, the unpaired electron is found in a HOMO consisting primarily of Mo 5p and 4d orbitals.

To the extent that the unpaired electron is localized on one atom, the anisotropy of the **g** tensor is determined by the angular momentum matrix elements between the HOMO and the lower excited-state orbitals, the energies of excitation (ΔE) to these states, and the value of the relevant spin–orbit coupling constant (ζ) (eq 3). Three of the anions have a value of ΔE that is 50–60% of that for the corresponding neutral complexes. The size of the matrix elements, which are difficult to evaluate, is important since, e.g., $[Mo^VO_2L^2]^-$ has the largest anisotropy of all the complexes, but ΔE is larger than ΔE for $[Mo^VO_2L^1]^-$ and $[Mo^VOSL^1]^-$. In the case of $[Mo^VOSL^1]^-$, the spin–orbit coupling constant is particularly important, since the unpaired electron is localized on S and the value of ζ for S is about half the value for Mo. As a result, even though ΔE for this complex is the smallest for all the complexes, its anisotropy is the smallest of the anions.

The large anisotropies in the **g** tensors observed with the anions, therefore, appear to be associated with the presence of a negative

Table 6. Mo Atom Basis A Primitive Gaussian Exponents and Contraction Coefficients

exponent	coefficient					
	1s	2s	3s	4s	5s	6s
8898.975 20	0.060 31	–0.019 25	–0.008 16	–0.003 18	–0.000 76	0.000 00
1346.693 00	0.363 52	–0.137 00	–0.058 97	–0.023 09	–0.005 51	0.000 00
295.628 76	0.656 52	–0.346 80	–0.159 93	–0.063 24	–0.015 13	0.000 00
37.964 58	0.121 06	0.775 98	0.619 38	0.268 12	0.065 12	0.000 00
15.608 90	–0.091 03	0.327 92	0.267 34	0.142 21	0.034 97	0.000 00
5.618 04	0.062 10	0.028 34	–0.973 46	–0.750 66	–0.196 77	0.000 00
2.482 53	–0.040 58	–0.012 53	–0.319 97	–0.299 64	–0.089 18	0.000 00
0.905 94	0.019 67	0.006 37	–0.017 74	0.951 75	0.373 90	0.000 00
0.377 77	–0.008 31	–0.002 83	0.004 22	0.396 00	0.235 31	0.000 00
0.075 34	0.002 34	0.000 80	–0.001 48	0.006 35	–0.615 85	0.000 00
0.028 87	0.000 00	0.000 00	0.000 00	0.000 00	0.000 00	1.000 00
	2p	3p	4p	5p		
548.863 88	0.082 68	–0.036 77	0.013 28	0.000 00		
127.392 68	0.425 92	–0.207 54	0.075 82	0.000 00		
37.712 84	0.583 56	–0.284 23	0.105 21	0.000 00		
12.659 60	0.082 07	0.428 98	–0.217 14	0.000 00		
4.770 07	0.007 45	0.671 48	–0.338 10	0.000 00		
1.350 50	–0.003 31	0.080 08	0.577 02	0.000 00		
0.474 12	0.001 41	–0.012 83	0.597 26	0.000 00		
0.080 00	0.000 00	0.000 00	0.000 00	1.000 00		
	3d	4d				
63.792 05	0.129 22	–0.035 01				
17.356 42	–0.494 27	–0.138 64				
5.210 95	–0.554 70	–0.096 62				
1.277 89	–0.077 86	0.458 25				
0.326 64	0.009 02	0.707 01				

Table 7. S Atom Basis B Primitive Gaussian Exponents and Contraction Coefficients

exponent	coefficient			
	1s	2s	3s	3s′
1201.458 40	0.064 62	–0.017 89	0.005 23	0.000 00
181.392 12	0.379 96	–0.122 82	0.036 09	0.000 00
39.404 80	0.649 04	–0.295 82	0.091 82	0.000 00
4.528 80	0.091 75	0.675 40	–0.305 18	0.000 00
1.754 94	–0.048 06	0.422 70	–0.283 25	0.000 00
0.381 43	0.017 32	0.017 14	0.764 90	0.000 00
0.138 79	0.000 00	0.000 00	0.000 00	1.000 00
	2p	3p	3p′	
54.644 07	0.101 77	–0.026 45	0.000 00	
12.122 90	0.457 14	–0.125 17	0.000 00	
3.206 50	0.578 17	–0.164 86	0.000 00	
0.863 27	0.070 78	0.233 89	0.000 00	
0.318 13	–0.001 29	0.567 46	0.000 00	
0.108 68	0.000 00	0.000 00	1.000 00	
	3d			
0.650 00	1.000 00			

Table 8. Si Atom Basis B Primitive Gaussian Exponents and Contraction Coefficients

exponent	coefficient			
	1s	2s	3s	3s′
909.234 87	0.065 32	–0.017 44	0.004 48	0.000 00
137.124 56	0.382 62	–0.118 93	0.030 75	0.000 00
29.714 81	0.648 13	–0.284 57	0.077 10	0.000 00
3.335 98	0.085 98	0.648 81	–0.241 29	0.000 00
1.251 26	–0.041 83	0.449 30	–0.276 37	0.000 00
0.226 39	0.014 03	0.016 91	0.741 07	0.000 00
0.082 40	0.000 00	0.000 00	0.000 00	1.000 00
	2p	3p	3p′	
37.881 76	0.107 17	–0.023 23	0.000 00	
8.304 60	0.462 87	–0.105 25	0.000 00	
2.120 79	0.580 27	–0.135 10	0.000 00	
0.447 80	0.082 00	0.239 97	0.000 00	
0.170 84	–0.022 13	0.552 39	0.000 00	
0.062 36	0.000 00	0.000 00	1.000 00	
	3d			
0.250 00	1.000 00			

Table 9. O Atom Basis A Promitive Gaussian Exponents and Contraction Coefficients

exponent	coefficient	
	1s	2s
281.866 58	0.068 09	–0.015 84
42.416 00	0.392 17	–0.102 56
9.095 62	0.640 79	–0.254 08
1.155 72	0.066 88	0.412 27
0.360 63	–0.019 46	0.694 97
	2p	
3.154 72	0.353 36	
0.543 50	0.798 19	

Table 10. N Atom Basis A Primitive Gaussian Exponents and Contraction Coefficients

exponent	coefficient	
	1s	2s
218.364 49	0.067 01	–0.014 80
32.598 89	0.389 78	–0.095 98
6.917 39	0.646 78	–0.246 70
0.855 41	0.065 50	0.399 75
0.268 04	–0.024 59	0.704 22
	2p	
2.292 17	0.348 39	
0.408 27	0.798 12	

Table 11. C Atom Basis A Primitive Gaussian Exponents and Contraction Coefficients

exponent	coefficient	
	1s	2s
153.172 26	0.069 81	–0.015 39
23.073 03	0.394 54	–0.095 93
4.923 29	0.639 86	–0.244 30
0.600 71	0.065 40	0.386 15
0.191 63	–0.020 46	0.713 74
	2p	
1.513 03	0.346 22	
0.272 51	0.798 48	

charge and two oxo groups. Replacement of an oxo (O_t) with a sulfido (S_t) considerably reduces the anisotropy, either by localizing the unpaired electron on S ($[Mo^VOSL^1]^-$) or by reducing the degree of coupling between the HOMO and the excited-state orbitals. Protonation of either the oxo (O_t) or sulfido (S_t) greatly reduces the anisotropy, mainly by increasing ΔE.

The agreement between the calculated and experimental values of the **g** tensors is, in general, surprisingly good, given the many approximations. The major discrepancies are with the $\mathbf{g}_{mid}$ value

Table 12. H Atom Basis A Primitive Gaussian Exponents and Contraction Coefficients

exponent	coefficient
	1s
1.919 087	0.274 37
0.290 226	0.821 26

of the anions, which in all cases, is too high. In addition, both g_{max} and g_{min} for *cis*-Mo^{V}O(SH)L^{2} are too low. For the other neutral species (and for $\langle g \rangle$ for Mo^{V}(Otms)L^{3}) the agreement is remarkably good. The discrepancies may be a result, in some cases, of the fact that 25–30% of the HOMO arises from atoms other than Mo (even though no single other atom contributes more than 1%). It should be pointed out that although the Mo–N bond lengths for N ligand atoms trans to the oxo O are invariably estimated too short by INDO, artificially increasing them to expected or *ab initio* Mo–N bond lengths does not change the calculated **g** tensor significantly. This is not surprising since the calculations show that atomic orbitals on the nitrogens contribute little to the HOMO.

The [Mo^{V}OSL^{1}]$^{-}$ structure is of particular importance, since a Mo^{V}OS center is proposed to be the origin of the very rapid EPR signal observed upon reduction of xanthine oxidase.[6–8] Furthermore, the complex [Ph$_4$P][Mo^{V}OSL^{1}] has been reported,[13] and while no suitable crystals were obtained for X-ray analysis, the compound was studied by EXAFS. Interestingly, no evidence could be found in the EXAFS results for a double bond (Mo=S), but the results did indicate the presence of one Mo=O and two or three long Mo—S bonds. Upon protonation, *cis*-Mo^{V}O(SH)-L^{1} is obtained, rather than *cis*-Mo^{V}(OH)SL^{1}, a result expected if the Mo—S$_t$ bond is essentially a single bond (a single-bonded Mo—S$_t$ is considerably more basic than a multiple-bonded Mo—O$_t$). Finally, there is no evidence from EXAFS for the presence of a short Mo—S bond in the species responsible for the very rapid EPR signal of xanthine oxidase,[32] and the rapid-signal species of the enzyme is formulated as MoO(SH), presumably arising by protonation of the very-rapid-signal species. Thus, the results reported here are in good agreement with the EXAFS results for both the enzyme and [Mo^{V}OSL^{1}]$^{-}$ and give additional support to the proposed structures of the species responsible for the catalytically important EPR signals of this enzyme. While the anisotropies of the very rapid and rapid EPR signals of xanthine oxidase are smaller than those of [Mo^{V}OSL^{1}]$^{-}$ and *cis*-Mo^{V}O(SH)L^{1}, the total ligand set in the enzyme remains unknown, but is almost certainly somewhat different from that in the complexes.[5,7] The results reported here emphasize the importance of the ligand in determining the details of the electronic structure and the values of the **g** tensors.

Table 13. *Ab Initio* Total Energies (hartrees) for Complexes at the Optimized Geometries

complex	energy (basis set)
Mo^{VI}O$_2$L^{1}	–5621.217 28 (B)
[Mo^{V}O$_2$L^{1}]$^{-}$	–5621.241 06 (B)
Mo^{VI}O$_2$L^{2}	–4977.476 84 (A)
[Mo^{V}O$_2$L^{2}]$^{-}$	–4977.485 26 (A)
	–4977.983 94 (B)
Mo^{V}O(OH)L^{2}	–4978.074 99 (A)
Mo^{V}O(Otms)L^{3}	–5726.362 26 (B)

The results indicate that *ab initio* and INDO methods may be of considerable use in predicting geometries and estimating EPR parameters for molecules of the size and complexity reported here and for the active sites of metal-containing enzymes.

Acknowledgment. This work was supported by NIH Grant GM-08437 (J.T.S.). Computer time provided by the Utah Supercomputing Institute and Department of Chemistry, University of Utah, is gratefully acknowledged. We wish to thank Dr. M. Feyereisen of Cray Research for the parallel version of DISCO and Prof. M. C. Zerner for the INDO code. J.N. and E.A.M. thank Prof. J. Simons of the University of Utah for helpful discussions.

Appendix

Our starting points for generating the atomic basis sets used in this work are the segmented contractions of Huzinaga[33] which use three exponent-optimized Gaussian primitives per shell. Examination of the exponents shows that, in the s shells, the smallest exponent in each shell overlaps the largest exponent in the next shell. Since in a generalized contraction a single primitive can appear in every basis function, the highest exponent primitive in each shell except 1s was deleted.

For first-row atoms it was further observed that if the number of 2p primitives was reduced from 3 to 2 and the 2s and 2p exponents were reoptimized, there was no degradation in the accuracy of predicted mimimum basis geometries of small test molecules such as CH$_3$OH. Unfortunately, this procedure failed when applied to the second-row atoms. The full set of Huzinaga 3p primitives and a split 3p valence shell were found to be required for even moderate agreement with the experimental S–C bond length in CH$_3$SH. Accordingly, only the ligand split valence basis (set B) was employed for complexes containing S.

Contraction coefficients were then obtained by performing atomic SCF calculations using the uncontracted primitive sets as modified above. The exponents and contraction coefficients are given in Tables 6–12. For an atom other than S or Si, basis set B is obtained from the tabulated basis set A by freeing the coefficients of the most diffuse s and p primitives in the case of a first-row atom or H and the most diffuse d in the case of Mo.

Total energies at the optimized geometries for the six complexes upon which *ab initio* calculations were performed are given in Table 13.

---

(32) Turner, N. A.; Bray, R. C.; Diakun, G. P. *Biochem. J.* **1989**, *260*, 563.

(33) *Gaussian Basis Sets for Molecular Calculations*; Huzinaga, S., Ed.; Elsevier: Amsterdam, 1984.